# Mechanical Strain Induces Distinct Human Scleral Fibroblast Lineages: Differential Roles in Cell Proliferation, Apoptosis, Migration, and Differentiation

Chen Qiu,[1,2] Minjie Chen,[1] Jing Yao,[1] Xinghuai Sun,[1–4] Jianjiang Xu,[1] Rong Zhang,[1,2] Xin Wang,[1] Gang Li,[1] and Shaohong Qian[1]

[1]Department of Ophthalmology, Eye and Ear, Nose, Throat Hospital, Shanghai Medical College, Fudan University, Shanghai, China
[2]Key Laboratory of Myopia, Ministry of Health, Fudan University, Shanghai, China
[3]State Key Laboratory of Medical Neurobiology, Institutes of Brain Science, Fudan University, Shanghai, China
[4]Shanghai Key Laboratory of Visual Impairment and Restoration, Fudan University, Shanghai, China

Correspondence: Shaohong Qian, Department of Ophthalmology, Eye and Ear, Nose, Throat Hospital, Shanghai Medical College, Fudan University, Shanghai 200031, China; qsh2304@163.com.

Submitted: January 13, 2018
Accepted: April 10, 2018

Citation: Qiu C, Chen M, Yao J, et al. Mechanical strain induces distinct human scleral fibroblast lineages: differential roles in cell proliferation, apoptosis, migration, and differentiation. *Invest Ophthalmol Vis Sci*. 2018;59:2401–2410. https://doi.org/10.1167/iovs.18-23855

**Purpose.** The purpose of this study was to explore the effect of mechanical strain on human scleral fibroblasts (HSFs) and compare cell behaviors of HSFs from distinct regions.

**Methods.** Primary HSFs were cultivated using a digestive protocol. Cells were seeded on collagen I–coated Bioflex plates, and a FX-5000 tension system was used to perform biaxial mechanical strain in vitro. We applied 10%, 0.5-Hz mechanical strain. Cell behaviors of peripapillary and periphery HSFs were compared after the strain. Edu imaging, Cell Counting Kit-8 assay, and cell cycle flow cytometry were conducted to analyze cell proliferation ability. For cell apoptosis, flow cytometry of Annexin V/propidium iodide, caspase 3 activity, and Western blot were performed. Immunofluorescence, real-time PCR, and Western blot were used to investigate cell differentiation. A migration assay was also performed.

**Results.** Under the mechanical strain of 10%, 0.5 Hz for 24 hours, the proliferation ability and cell apoptosis of peripapillary HSFs did not have a significant change. The expression of alpha-smooth muscle actin (α-SMA) slightly decreased. However, increased cell proliferation, attenuated cell apoptosis and more expression of α-SMA were shown in the periphery HSFs under the same condition. The migration rate was also increased for periphery HSFs, whereas it kept almost the same for peripapillary HSFs under 10%, 0.5-Hz strain for 8 hours.

**Conclusions.** Mechanical strain affected the cell behaviors of HSFs. The different performance of cells from distinct regions may suggest familial linages of HSFs, probably induced by mechanical strain.

Keywords: mechanical strain, sclera, fibroblasts, cell behavior, glaucoma

Glaucomatous damage is the direct result from degeneration of retinal ganglion cell (RGC) axons. IOP is one of the most important risk factors. Studies in recent years have also identified lower intracranial pressures (ICPs) in open-angle glaucoma patients, especially those with normative IOP.[1–3] The strain caused by IOP and ICP, resulting in the translaminar pressure and hoop-like strain, may exert a direct impact on the optic nerve head (ONH). Excessive stresses and strains on the ONH may block axoplasmic transport, hemodynamics, and nutrient distribution within the ONH. Hence, the ONH behaviors influenced retinal RGC survival of glaucoma patients.

The laminar cribrosa (LC) and peripapillary sclera (PPS) are the main load-bearing connective tissues of the ONH. Experimental and computational models have especially confirmed the vital role of the biomechanics of PPS on glaucoma damage and progression.[4–7] For instance, when IOP changed, the PPS functioned by altering the movement of LC, either posteriorly or anteriorly.[8,9] Although the biomechanical properties of PPS tissue have been abundantly investigated, the biomolecular alterations induced by mechanical strain in this particular region have not been well documented yet.

The sclera is composed of scleral fibroblasts and its extracellular matrix (ECM), mainly referred to collagen I and collagen IV. The eyeball is not an intact global wall, as the axons of RGCs, central retinal artery, and central retinal vein transverse the LC to form the optic nerve. PPS supported more strain than other parts of human eyes.[10] The anatomical differences between the PPS and non-PPS regions may contribute to varying tissue bearing load and distinct properties of scleral fibroblasts and ECM in these regions.

Mechanical load may affect cell morphology and behaviors, including cell proliferation, apoptosis, migration, and differentiation.[11–13] Here, we aimed to compare PPS fibroblasts and periphery fibroblasts and explore the effects of mechanical strain on the cell behaviors of human scleral fibroblasts (HSFs).

## Materials and Methods

### Cell Cultivation

All human eyes were obtained from the Eye Bank of Eye and Ear, Nose, Throat (EENT) Hospital of Fudan University within 24 hours post mortem. Consent to use for research purpose

was made before the experiment. The study was approved by Institutional Review Board and Ethics Committee of EENT Hospital of Fudan University. According to the medical history, all donors were free of any history of ocular disease other than cataracts. A total of 15 human eyes from nine donors were enrolled in this study, among which 5 eyes were used for cell line cultivation. Primary HSFs were cultured following a collagenase digestion protocol. Briefly, the PPS (2-mm scleral band from the ONH[14]) and periphery sclera were carefully dissected from the donor eyes and were then digested by collagenase NB4 (Serva, Heidelberg, Germany) overnight at 37°C. After filtration (70 μm; Falcon; BD, Franklin Lakes, NJ, USA) and resuspension, HSFs were cultured in Dulbecco's modified Eagle's medium (DMEM; Gibco, Grand Island, NY, USA) containing 20% FBS and 1% penicillin-streptomycin (Hyclone, South Logan, UT, USA) under the normal condition (37°C, 5% $CO_2$ in a humidified atmosphere). After 1 week, growth media were exchanged every 3 days. HSFs after passage 1 were grown in DMEM with 15% FBS and 1% penicillin-streptomycin. Cells between passage 4 and 7 were used for experiments.

## Mechanical Strain

The Flexcell FX-5000 tension system (Flexcell International Corporation, Burlington, NC, USA) was a computer-controlled system, producing various mechanical force. HSFs ($2–5 \times 10^5$) were seeded into the six-well collagen I-coated Bioflex plates (Flexcell International Corporation). After 24-hour culturing with DMEM containing 10% FBS and 24-hour cultivation with serum-free DMEM, cells were replenished with media containing 1% FBS before mechanical strain. HSFs cultured on the flexible membrane were set as the unloaded control or subjected to the biaxial mechanical force that may partially represent elevated IOP. A sinusoidal cyclic mechanical strain with a frequency of 0.5 Hz and a maximum elongation of 10% was applied, respectively, according to our preliminary work.

## Cell Counting Kit Assay

After resuspension, approximately $1 \times 10^4$ cells were incubated in 96-well plates for 24 hours. Cell Counting Kit-8 (CCK-8; Dojindo, Kumamoto, Japan) was used for cell viability assays, following the manufacturer's protocol. The absorbance was read at 450 nm by a microplate reader (BioTek; Synergy HTX, Winooski, VT, USA).

## 5′-Ethynyl-2′Deoxyuridine Imaging

HSFs receiving mechanical stimuli or as the unloaded control (mechanical stimulated versus unstimulated) were transferred into 96-well plates and cultured at 37°C overnight. 5′-Ethynl-2′deoxyuridine (Edu; 10 μM) was incubated for 4 hours before cells were fixed and permeabilized. Click-iT Edu Alexa Flour 488 imaging kit (Life Technologies, Eugene, OR, USA) was used according to the manufacturer's instructions. Images were captured by using light microscopy (Nikon Eclipse Ti-S; Nikon, Tokyo, Japan).

## Cell Cycle of Flow Cytometry

Mechanical stimulated and unstimulated HSFs were resuspended and washed twice with precooled PBS (4°C), respectively. Then cells were fixed with 75% ethanol overnight at −20°C. Before the machine test (Gallios; Beckman, Brea, CA, USA), cell were centrifuged and washed with PBS and stain butter (BD Pharmingen, San Diego, CA, USA) and then exposed to propidium iodide (PI)/RNase staining buffer (BD Pharmingen) in the dark for 15 minutes. We analyzed the data of the cell cycle with Modfit software (Verity Software House, Topsham, ME, USA).

## Annexin V Alexa Flour 488/PI Dual Staining Assay

The Dead Cell Apoptosis Kit with Annexin V Alexa Flour 488 and PI kit (Life Technologies) was developed to detect apoptotic and dead cells. In brief, $1 \times 10^6$ cells were resuspended in 100 μL 1× binding buffer. PI and fluorescein isothiocyanate (FITC) Annexin V staining was carried out for 15 minutes at room temperature in the dark. Cell apoptosis was analyzed using FACScan flow cytometry (Gallios; Beckman) and FlowJo software (BD). Apoptotic cells were stained positively for Annexin V but negatively for PI staining.

## Caspase 3 Activity Assay

Caspase 3 activity was measured according to the manufacturer's introduction (Boyongtime, Shanghai, China). In brief, cells, with or without mechanical stimuli, were carefully harvested and lysed at a concentration of $2 \times 10^6$/100 μL, incubated on ice for 15 minutes, and centrifuged at 16,000*g* for 15 minutes. After reaction with 10 μL Ac-DEVD-pNA (2 mM) at 37°C for 1 hour, caspase 3 activity was quantified with a microplate reader (BioTek; Synergy HTX) by reading at 405 nm.

## Immunocytochemistry/Immunofluorescence Analysis

HSFs were seeded into 24-well plates containing coverslips coated with 0.1% gelatin (Sangon Biotech, Shanghai, China). Cells were fixed at room temperature for 15 minutes in 4% formaldehyde PBS and then washed twice with PBS, followed by permeabilization with 0.1% Triton X-100 in PBS for 10 minutes and blocking with 5% BSA (Sigma-Aldrich Corp., St. Louis, MO, USA) in PBS for 1 hour. Diluted primary antibodies (vementin, keratin, and alpha-smooth muscle actin (α-SMA); Abcam, Cambridge, UK) in 1% BSA were incubated overnight at 4°C. Secondary antibodies (Alexa 488 and Cy3; Thermo Fisher Scientific, Waltham, MA, USA) were incubated for 1 hour at room temperature. All images were captured by confocal fluorescence microscopy (Leica SP8; Leica, Berlin, Germany).

## Quantitative RT-PCR

Total RNA was isolated using TRIzol (Invitrogen, Carlsbad, CA, USA). mRNA was reverse-transcribed to cDNA using the commercially available PrimeScript RT reagent kit (Takara, Dalian, China). Real-time PCR was conducted with SYBR Premix Ex Taq (Takara) using the ABI ViiA7 Real Time PCR system (Thermo Lifetech, Carlsbad, CA, USA) under the following conditions: 95°C for 30 seconds and then 50 cycles of 95°C for 5 seconds and 60°C for 30 seconds. Primer sequences were as follows: *GAPDH* (housekeeping gene) 5′-ACAACTTTGGTATCGTGGAAGG-3′ and 5′-GCCATCACGCCACAGTTTC-3′; *α-SMA* 5′-CCGGGACTAAGACGGGAATC-3′ and 5′-CACCATCACCCCCTGATGTC-3′.

## Western Blot

Tissues and cells were lysed in radio-immunoprecipitation assay (RIPA) buffer (Biocolor, Shanghai, China) containing protease inhibitor phenylmethanesulfonyl fluoride (PMSF) (Biosharp, Hefei, China). Samples were resolved in SDS-PAGE (Takara) and transferred onto nitrocellulose blotting membranes (GE Healthcare Life Science, Freiburg, Germany). Primary antibodies were as follows: anti–α-SMA (1:1000;

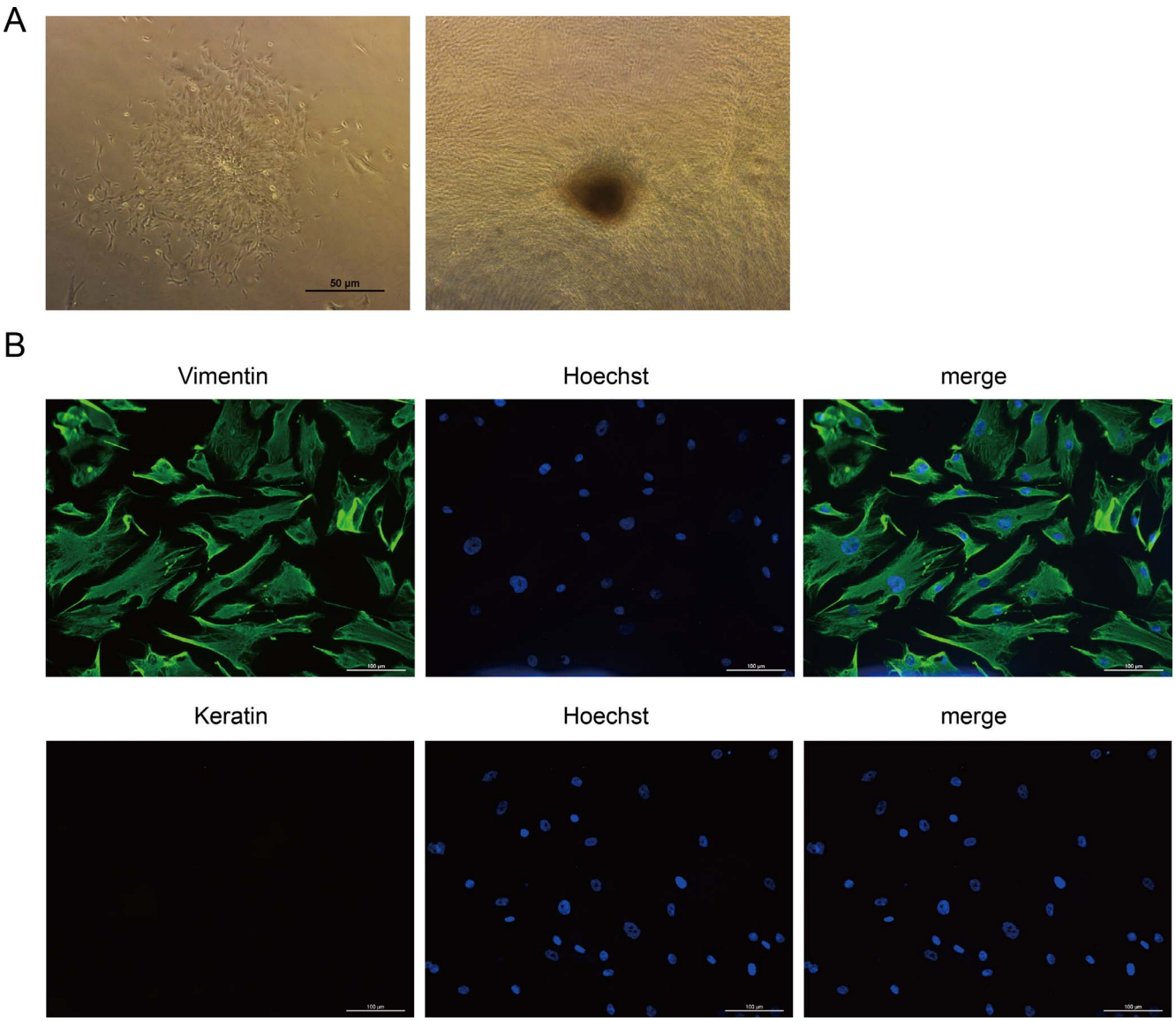


FIGURE 1. Isolation and identification of primary HSFs. (**A**) The spindle-shape cells were primary HSFs cultivated at days 8 and 14, respectively, using a collagenase protocol. *Scale bar*: 50 μm. (**B**) Confocal immunofluorescent images showed the identification of HSFs at passage 4: positive staining for vimentin (*green*) and negative for keratin were fibroblasts. Nuclei were stained with Hoechst (*blue*). *Scale bar*: 100 μm.

Abcam), anti-Caspase 3 (1:1000; Cell Signaling Technology, Boston, MA, USA), and anti-GAPDH (1:10,000; Bioworld, St. Louis Park, MN, USA) or anti–β-tubulin (1:1000; Abcam). GAPDH or β-tubulin was used as the loading control. Horseradish peroxidase (HRP)-conjugated secondary antibody (1:3000; Cell Signaling Technology) was incubated for 1 hour at room temperature. Super Signal West Femto Substrate Trial Kit (ThermoFisher) was used for chemiluminescence detection. The immunoreactive bands were analyzed in triplicate with Image J software (National Institutes of Health, Bethesda, MD, USA).

### Migration Assay

For the migration assay, cells ($2.5 \times 10^5$) were seeded into six-well culture plates. After a 24-hour incubation with DMEM containing 10% FBS, the growth media were exchanged with serum-free DMEM. Distance between cells borders of each scratch side was monitored every 2 hours using Leica DMI 6000B microscopy, with exactly the same sites of plates.

### Statistical Analyses

All experiments were repeated at least three times. Statistical analyses were performed using SPSS version 19.0 (SPSS, Inc., Chicago, IL, USA). Student's *t*-test or 1-way ANOVA was performed to compare the difference. $P < 0.05$ was set to be statistically significant.

## RESULTS

### Isolation and Identification of Primary HSFs

The primary HSFs were cultivated in a digestive protocol (Fig. 1A). Five pairs of cell lines (both periphery and PPS scleral fibroblasts) were obtained from four human donors (Table). The spindle-shaped cells were typically fibroblasts and primary HSFs could grow into confluence in about half a month. To identify the cells as scleral fibroblasts, immunofluorescence imaging was done. As shown in Figure 1B, vimentin (+)/

Table. Demographic Information of Human Eyes

| No. | Age, y | Race | Sex | Eye | Application |
|---|---|---|---|---|---|
| 1 | 45 | Han | Female | Right | Cell cultivation |
| 2 | 68 | Han | Female | Left | Cell cultivation |
| 3 | 40 | Han | Male | Right/left | Cell cultivation |
| 4 | 69 | Han | Male | Left | Cell cultivation |
| 5 | 57 | Han | Male | Right/left | qPCR, Western blot |
| 6 | 46 | Han | Male | Right/left | qPCR |
| 7 | 67 | Han | Male | Right/left | qPCR, Western blot |
| 8 | 52 | Han | Female | Right/left | qPCR, Western blot |
| 9 | 78 | Han | Male | Right/left | qPCR, Western blot |

qPCR, quantitative PCR.

keratin(–) cells were considered as HSFs. After mechanical strain, cytoskeleton staining showed that the cells were still fibroblasts/myofibroblasts, as the obviously positive staining of α-SMA (Supplementary Fig. S1).

## Differences Between Periphery Fibroblasts and PPS Fibroblasts Without Strain

The classic difference between periphery fibroblasts (left) and PPS fibroblasts (right) in morphology was shown in Figure 2A. PPS fibroblasts were more likely to assemble in small clusters in the culture dishes. In fact, PPS fibroblasts grew faster than its periphery fibroblasts, as it was usually

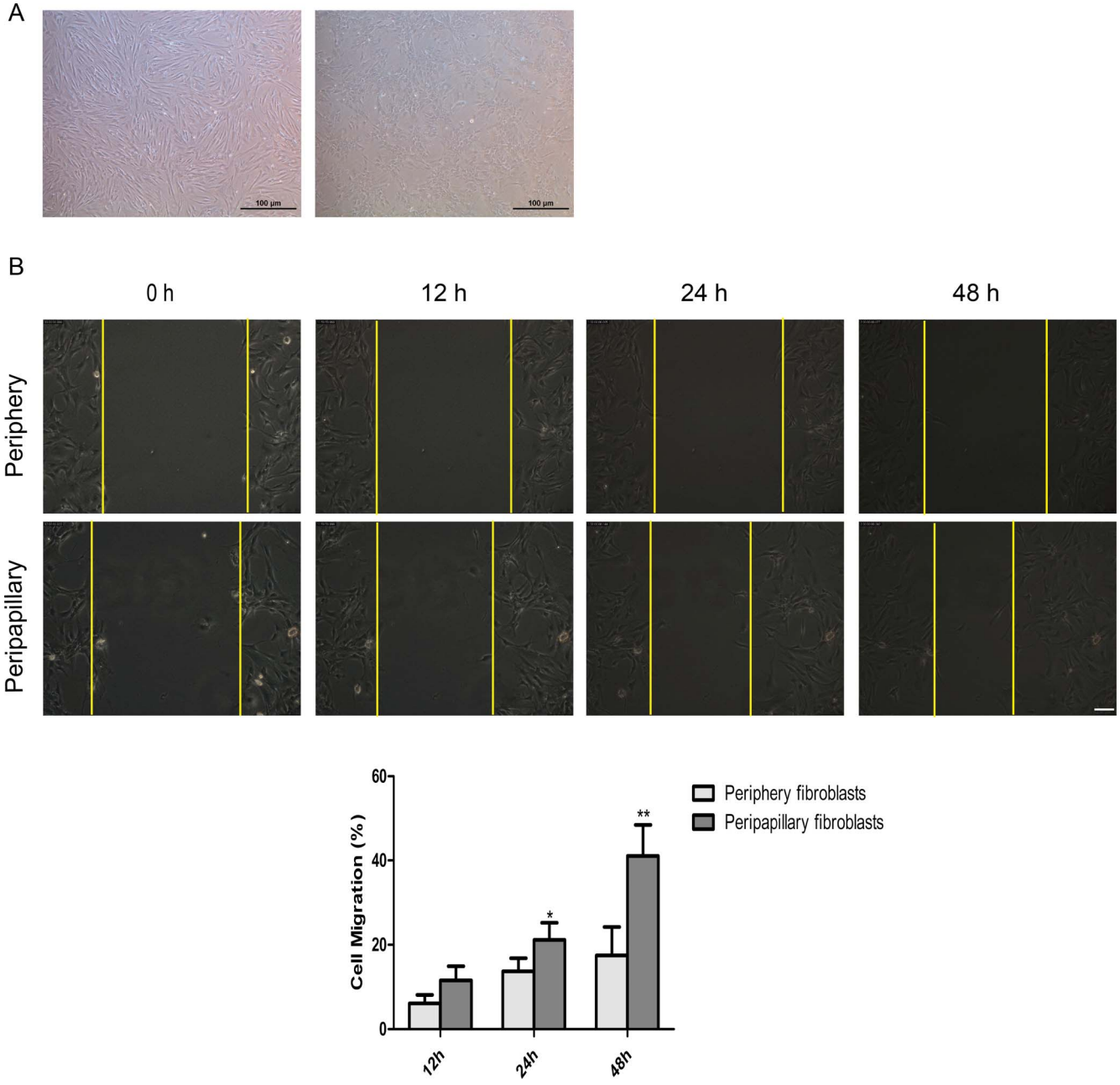


Figure 2. Differences between periphery fibroblasts and PPS fibroblasts without strain. (**A**) The classic, morphologic differences between periphery fibroblasts (*left*) and PPS fibroblasts (*right*) at passage 3 from the same eye. *Scale bar*: 100 μm. (**B**) Comparison and quantification of cell migration between periphery fibroblasts and PPS fibroblasts from the same eye ($n = 3$). PPS fibroblasts migrated faster than periphery fibroblasts. *$P < 0.05$; **$0.0001 < P < 0.01$. *Scale bar*: 100 μm.

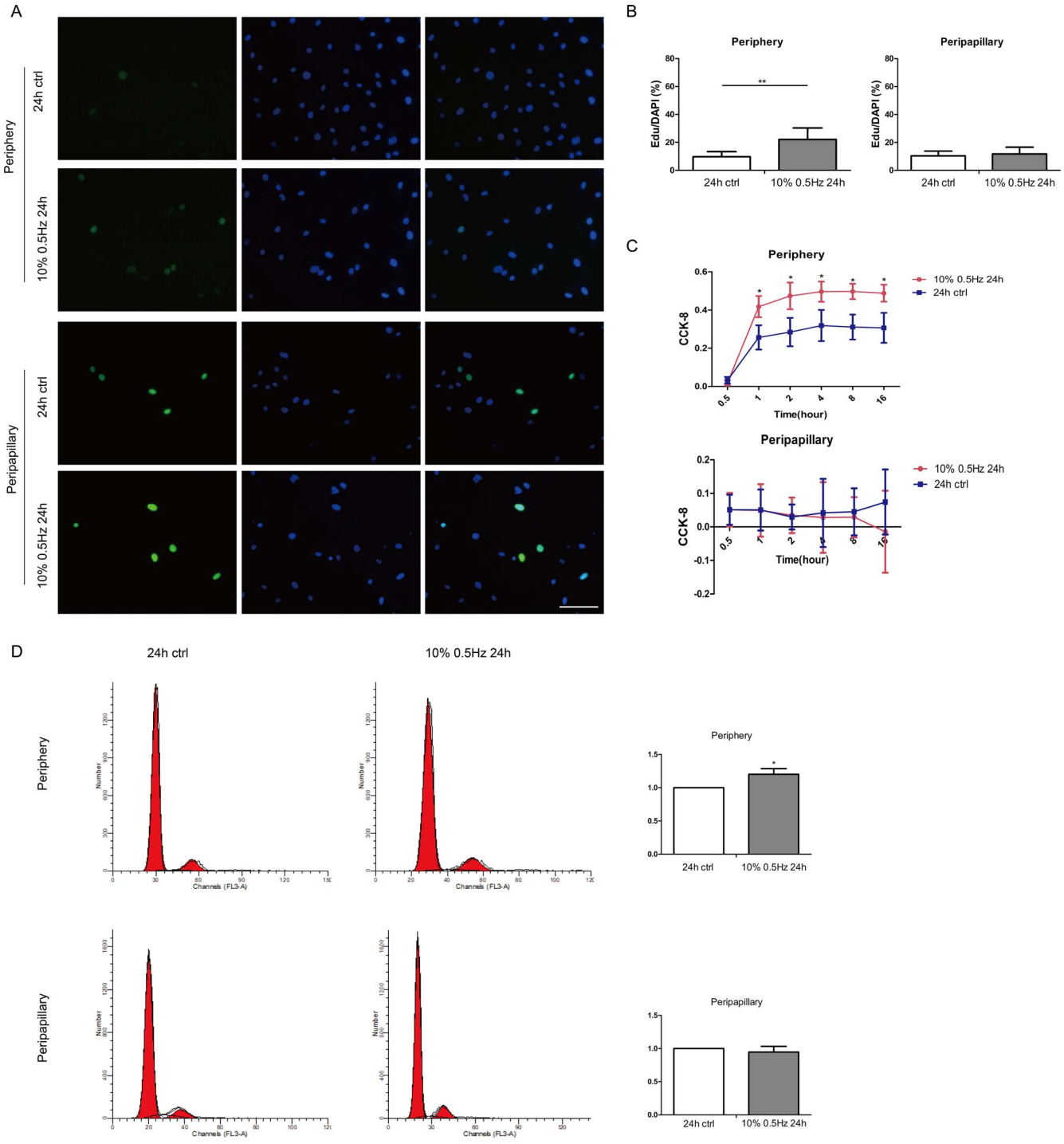


**Figure 3.** Effects of mechanical stimuli on the proliferation of HSFs. Periphery and PPS fibroblasts were subjected to 10% cyclic strain at 0.5 Hz or unloaded for 24 hours, respectively. (**A**) The Edu staining of periphery and PPS fibroblasts at static condition and after strain, respectively. (**B**) Quantification of the proportion of positive Edu staining ($n = 3$). After the mechanical stain, increased staining was shown in periphery fibroblasts, whereas the Edu staining of PPS fibroblasts were similar. (**C**) The Cell Counting Kit-8 assay of periphery fibroblasts and PPS fibroblasts with or without strain, respectively ($n = 4$). (**D**) Cell cycle conducted by flow cytometry and the quantification analysis ($n = 4$). Results were demonstrated as means ± SD of three separate experiments. *$P < 0.05$; **$0.0001 < P < 0.01$. *Scale bar*: 100 µm.

easier for PPS fibroblasts to reach confluence (data not shown). Furthermore, HSFs from PPS migrated faster than cells from periphery sclera (Fig. 2B). The differences initiated our speculations that HSFs from different regions might be distinct familial linages.

## Effects of Mechanical Stimuli on the Proliferation of HSFs

Mechanical strain was crucial to cell destiny. To investigate the effects of mechanical loading on HSFs proliferation ability, we conducted Edu cocktail imaging, CCK-8 assays, and flow

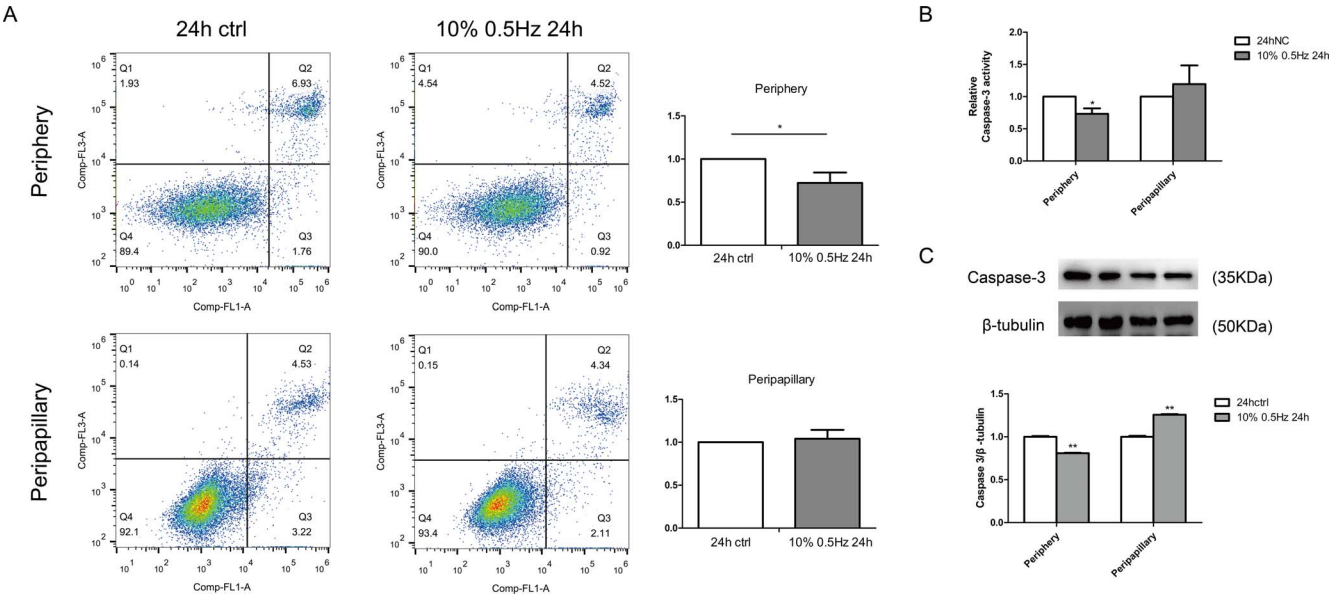


**Figure 4.** Effects of mechanical stimuli on cell apoptosis of HSFs. Periphery and PPS fibroblasts were subjected to 10% cyclic strain at 0.5 Hz for 24 hours. (**A**) The mechanical strain attenuated cell apoptosis of periphery fibroblasts, but it did not affect that of PPS fibroblasts, shown by flow cytometry and its quantification ($n = 4$). (**B**, **C**) Caspase-3 activity assay ($n = 3$) and Western blot analysis ($n = 3$) for periphery fibroblasts and PPS fibroblasts, with or without strain. Relative levels of Caspase-3 protein were determined by normalizing to tubulin. Results were shown as means ± SD of three replicates. *$P < 0.05$; **$0.0001 < P < 0.01$.

cytometry to assess cell cycle. Edu imaging showed that the proliferation ability of PPS fibroblasts did not have obvious change when subjected to 10% strain with a frequency of 0.5 Hz for 24 hours. The number of positive staining cells were similar with the unloaded control. However, periphery fibroblasts revealed a significant increase in the number of positive staining cells after mechanical loading (Figs. 3A, 3B). For cell viability, the CCK-8 assay confirmed an upregulated activity of periphery fibroblasts after the strain, while no significant change in that of PPS fibroblasts (Fig. 3C). In addition, flow cytometry was conducted to determine the phase of cell cycle. For periphery fibroblasts, there was a slight decrease in G1 phase and a significant increase in G2 phase and S phase. However, PPS fibroblasts almost retained equally for the resting and stretched cells (Fig. 3D). These findings constantly suggested that mechanical strain increased cell proliferation ability in periphery scleral fibroblasts, but not PPS fibroblasts.

## Effects of Mechanical Stimuli on Cell Apoptosis of HSFs

To determine whether mechanical stimulation affected cell apoptosis of HSFs, we first performed Annexin V/PI staining and analyzed with flow cytometry. Similarly, different responses to mechanical loading were demonstrated between periphery and PPS fibroblasts. Mechanical strain tended to attenuate the apoptosis of periphery fibroblasts but could not retard that of PPS fibroblasts (Fig. 4A). To further prove it, the protein level of apoptosis relating genes should be examined. Caspase 3 is a known classic apoptosis relating protein. Thus, cell apoptosis in protein level could be reflected by caspase-3 activity assay and Western blot. There was a significant decrease of caspase-3 activity in the strain-loading periphery HSFs compared with the control group. However, no significance was obtained regarding caspase-3 activity in the PPS fibroblasts, with or without mechanical stimulation (Fig. 4B). Western blot analysis of protein caspase-3 (Fig. 4C) was in line with the activity assay (Fig. 4B). Taken together, the results indicated that mechanical loading also affected cell apoptosis. A proper amount of mechanical strain could activate the "inert" fibroblasts, protecting them from apoptosis. On the contrary, this type of cell death was initiated when reached the maximum cell tolerance, especially for the activated PPS fibroblasts.

## Differences of Cell Migration Between PPS Fibroblasts and Periphery Fibroblasts Under Mechanical Stimuli

Cell migration assay was performed to observe cell mobility. Without external strain, PPS fibrobasts migrated significantly faster than periphery fibroblasts from the same human eyes, as previously mentioned. Under mechanical strain (10%, 0.5 Hz for 8 hours), the migration rate was significantly different between static and stretched periphery fibroblasts. To the contrary, for PPS fibroblasts, the speed of cell migration slightly slowed down but had no significant difference after mechanical loading (Fig. 5). In fact, HSFs are more likely to assemble in PPS than in other regions, as reflected by the number of digestive cells during cell cultivation (data not shown). We speculated PPS fibroblasts receive more dose of mechanical stimuli, as PPS was supposed to endure more stimulation during IOP fluctuation. Taken together, low dose of accumulated mechanical strain may enhance cell migration, while overdose of strain may eliminate the effect or even inhibit cell migration.

## Expression of α-SMA With or Without Mechanical Strain

To address why cell behaviors were different from distinct regions, we investigated the differentiation degree of HSFs. A higher gene and protein expression of α-SMA was shown in the PPS than in periphery sclera of human tissues (Figs. 6A–6C). Additionally, immunofluorescence imaging of fibroblasts from PPS and periphery sclera were in accordance with the results

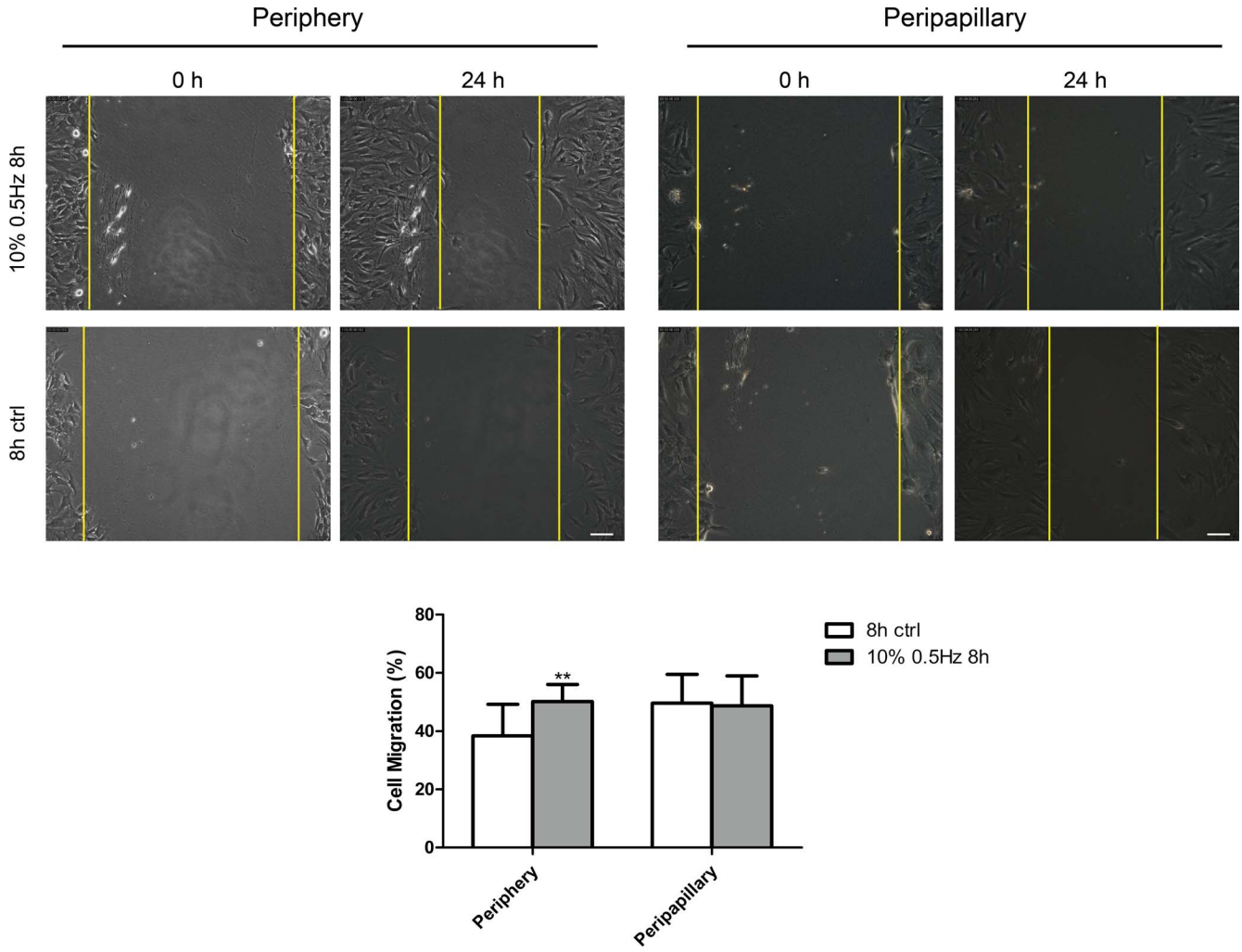


FIGURE 5. Cell migration differences between PPS and periphery fibroblasts under mechanical stimuli ($n = 3$). The migration rate of periphery fibroblasts increased after 10%, 0.5-Hz strain for 8 hours. The mechanical strain did not affect cell motility of PPS fibroblasts under the same condition. **$0.0001 < P < 0.01$. *Scale bar*: 100 μm.

of tissue samples (Fig. 6D), with more α-SMA expression in PPS fibroblasts. Herein, we confirmed a distinct differentiation state of scleral fibroblasts between PPS and periphery sclera. It was worth noticing that there was 20-fold more α-SMA protein in the PPS compared with the peripheral sclera tissues; however, the ratio was not preserved in cell lines.

We further investigated force-induced cell differentiation on both kinds of cells. Concordantly, mechanical strain stimulated α-SMA expression in periphery fibroblasts, both in gene and protein levels. Unexpectedly, the expression of α-SMA was slightly decreased in PPS fibroblasts, although without significance (Figs. 7A, 7B). Interestingly, the expression of α-SMA was in accordance to cell behaviors, including cell proliferation, apoptosis and migration. Collectively, strain–stimulated fibroblast-to-myofibroblast transition may somehow affect cell behaviors of the HSFs.

## Discussion

In this study, we aimed to explore the difference between PPS fibroblasts and periphery fibroblasts and to investigate the effect of mechanical strain on HSFs. The results confirmed the influence of mechanical strain on the sclera. Our data revealed that HSFs resided in different regions held varied characteristics in cell proliferation, apoptosis, migration, and differentiation under mechanical stimulation. Mechanical forces may promote cell proliferation, migration, and differentiation, but inhibited cell apoptosis of fibroblasts from periphery sclera. Nevertheless, PPS fibroblasts revealed lower sensitivity to the mechanical stimulation. Our findings thus may indicate a potential different familial lineage of HSFs, probably induced by mechanical stimuli.

Mechanical strain is a known inducer of ECM remodeling in a number of tissues and organs, such as skin,[15] lung tissue,[11,16] bone,[17] and vascular systems.[18] Alterations include cell reorientation, matrix composition, collagen, and elastin realignment.[5,19,20] The strain may also change the destiny of kinds of cells. Stretch influences cell morphology and behaviors, including proliferation, apoptosis, migration, and differentiation. To evaluate the effects of elevated IOP on sclera in glaucoma, the Flexcell-5000 tension system was used in vitro to mimic the mechanical stimulation induced by ocular hypertension. Consistently, mechanical loading could also alter the cell behaviors of HSFs. The distinct cell behaviors between PPS and periphery fibroblasts and their sensitivity to mechanical strain implied sclera from different regions were subjected to varying degrees of tension, which was in agreement with the biomechanical tests of sclera as previously reported.[10,19]

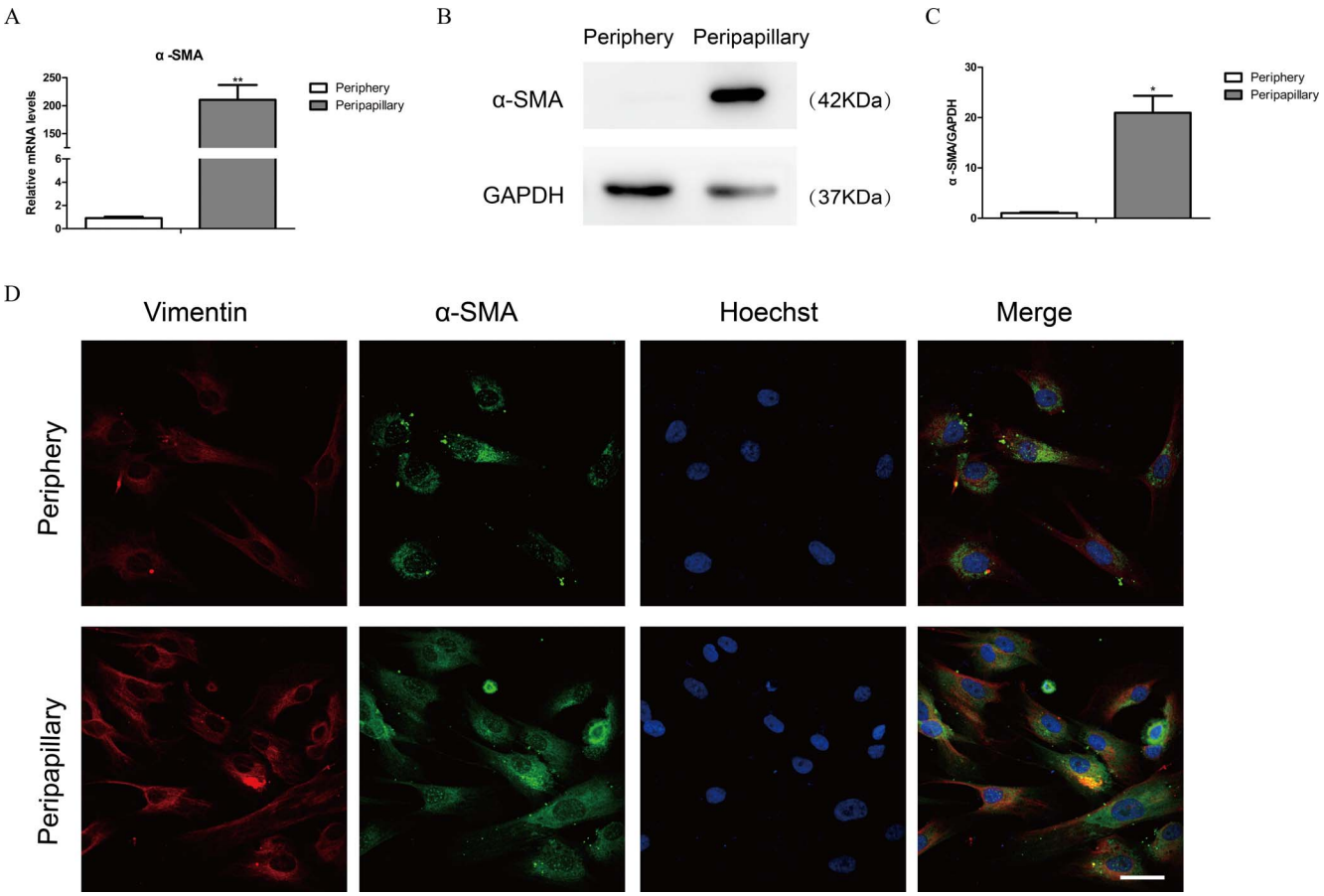


**Figure 6.** Expression of α-SMA in human eyes and primary cultivated HSFs. (**A**) The mRNA expression of α-SMA in periphery sclera and PPS from the same human eyes ($n = 6$). (**B**, **C**) Western blot showed the protein level of α-SMA in periphery sclera and PPS and the quantification analysis ($n = 4$). (**D**) Confocal immunofluorescent images of vimentin (*red*), α-SMA (*green*), and nuclei (*blue*) of primary HSFs. GAPDH was used as the loading control. Results were means ± SD of three replicates. $^{*}P < 0.05$; $^{**}0.0001 < P < 0.01$. *Scale bar*: 50 μm.

α-SMA is a hallmark of myofibroblasts. Higher levels of α-SMA expression indicates more myofibroblast differentiation. With proper external irritation, the "inert" fibroblasts could change their phenotype to the "active" myofibroblasts. Literatures also indicated that biomechanical factors are one of the major determinants of fibroblast-to-myofibroblast transition.[21] Both in vivo and in vitro, mechanical strain produced and prolonged myofibroblast persistence[14,16] or reduced myofibroblast differentiation.[12] In recent years, biomechanical tests have confirmed a stiffer tissue of PPS compared with other regions.[19,22,23] Our data that tissues and cells from PPS possessing more gene and protein expression of α-SMA were in line with the aforementioned literature. According to the anatomy of human sclera, PPS is at the edge of the incomplete spherical globe, enduring more tension from IOP. The disparate differentiation state of HSFs between PPS and periphery sclera may herein reflect a mechanical adaption, relating to the tension they sensed. Additionally, according to the results of migration tests, we may speculate that strain-induced cell motility resulted in HSFs reorientation. A larger proportion of myofibroblasts surrounding the optic disc implied more secretion of collagens and matrix metalloproteinases or tissue inhibitor of metalloproteinases, satisfying the remodeling of the scleral ECM. The absence of external strain

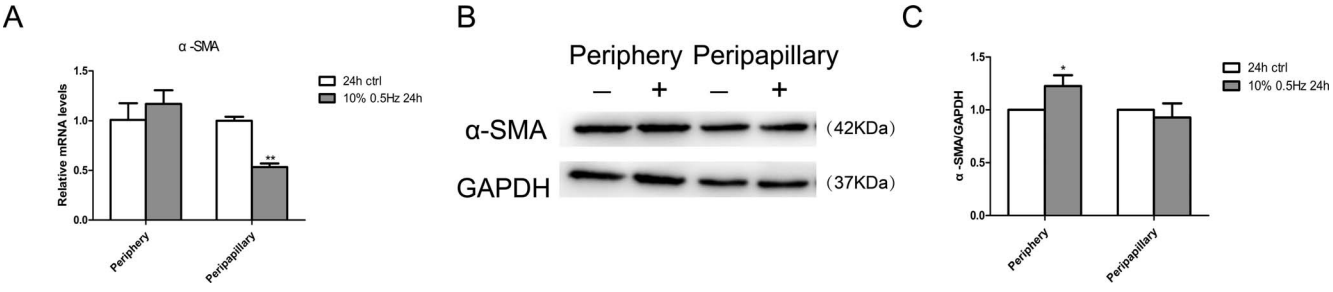


**Figure 7.** Expression of α-SMA in HSFs after mechanical strain. Periphery and PPS fibroblasts were subjected to 10% cyclic strain at 0.5 Hz for 24 hours. (**A**) The mRNA expression of α-SMA in periphery fibroblasts and PPS fibroblasts with or without strain, respectively ($n = 3$). (**B**, **C**) The protein level of α-SMA and the quantification analysis ($n = 3$). *GAPDH* was set as the housekeeping gene. Results were shown as means ± SD of three replicate. $^{*}P < 0.05$; $^{**}0.0001 < P < 0.01$.

may attenuate α-SMA expression, as PPS and periphery fibroblasts in vitro did not preserve the fold changes in sclera tissues in our study.

Cytoskeleton sensed the external strain and transduced the mechanical signs into biochemical messages. How cell functioned highly depended on the applied strain and the stimulating time. There were sparse literatures regarding to the effects of mechanical stimulation on scleral fibroblasts. One study demonstrated that in seven of the eight human eyes, α-SMA expression was upregulated in PPS fibroblasts under 1% and 4%, 0.5-Hz mechanical strain for 24 hours.[14] However, the last sample with a highest α-SMA expression at baseline revealed an opposite result under the same condition. In this situation, mechanical stress attenuated myofibroblasts differentiation. The researchers postulated that the baseline α-SMA expression might affect strain-stimulated myofibroblast differentiation. A possible mechanism would be that mechanical stimulation had an accumulation effect. The external mechanical stimulation facilitated the transition of the "inert" periphery fibroblasts into an active state, as fibroblasts in this region experienced the strain at a low level. To the contrary, in the PPS, most of the fibroblasts may have already turned into myofibroblasts. The "ceiling effect" may retard further upregulation of α-SMA in PPS fibroblasts, thus limiting myofibroblasts transition. Similarly, fibroblast/myofibroblast ratio also affected the potential capacity of cell proliferation, apoptosis, and migration.

Some research demonstrated that phosphorylation of the myosin light chain (MLC) is associated with cell contractility. Myosin/actomyosin were motivated to contract when more MLC phosphorylated. Rho, a small GTP-binding protein, is a molecular switch that modulate cell tension and actin fibrils. The activation of Rho not only led to actin polymerization and MLC phosphorylation, but also promoted myofibroblast differentiation.[23] Qu et al. showed that the phosphorylation of MLC was in accordance with the expression of α-SMA.[14] Furthermore, inhibition of MLC phosphorylation also prevented α-SMA expression,[24] suggesting the role of MLC in modulating cell differentiation. Therefore, we suspected that fibroblast-to-myofibroblast transition might predict cell motility. Our data revealed that PPS fibroblasts moved faster than the periphery fibroblasts. However, the periphery fibroblasts had greater potential to increase migration rate while the cell motility of PPS fibroblasts did not change much after 8 hours of 10%, 0.5-Hz strain. The motility of PPS cells even tended to slow down though without significance. Consistently, a decreased α-SMA expression in the PPS fibroblasts and an increased α-SMA expression in the periphery fibroblasts was noted after the strain in the study, suggesting that the expression of α-SMA and its alterations after mechanical stretch may affect cell migration.

In this study, mechanical load inhibited the activity and even cause cell apoptosis of scleral fibroblasts in PPS, whereas it promoted cell proliferation and attenuated apoptosis of periphery fibroblasts. Intercellular calcium may to some extent explain the phenomena. According to Liu et al.,[25] stress-stimulated calcium channel opening may affect cell behaviors. Short-term overloaded mechanical stimulation promoted proliferation and differentiation of cells rather than apoptosis via elevated intracellular calcium. However, long-term overloading may cause apoptosis of the osteoblasts due to the overloading of intracellular calcium. The accumulated effects of mechanical strain may determine cell proliferation and apoptosis. In short, cell destiny was closely related to their cumulative mechanical strain.

However, there were several limitations of the study. We applied biaxial plane strain on the HSFs by the Flexcell-5000 tension system. In fact, the mechanical environment of HSFs was complicated as compressive loads may also occurred in vivo. Therefore, the strain applied in this study could only mimic and partially represent the elevated IOP in vivo. Additionally, IOP fluctuation may also affect the strain cell sensed, but the frequency of strain was only set at 0.5 Hz in the study. Multiple levels of strain frequencies should be explored in the future. Furthermore, the molecular mechanisms and signaling pathways would be investigated to elucidate how mechanical strain affect the cell behaviors of HSFs.

In summary, the data demonstrated mechanical loading brought about alterations in cell behaviors, such as proliferation, apoptosis, migration, and differentiation. HSFs from different regions showed disparate response under the same condition. A proper amount of mechanical strain could activate the "inert" fibroblasts, whereas an overdose of strain may desensitize HSFs to mechanical stimulation.

## *Acknowledgments*

The authors thank Chuandong Wang, Shengzhou Shan, and Jiali Ruan for research assistance in the study.

Supported in part by Natural Science Foundation of Shanghai (18ZR1406000), State Key Program of National Natural Science Foundation of China Grant 81430007, International Science & Technology Cooperation Program of China Grant 2015DFA31340, and National Natural Science Foundation of China Grants 81300792, 81401533, and 81500723.

Disclosure: **C. Qiu**, None; **M. Chen**, None; **J. Yao**, None; **X. Sun**, None; **J. Xu**, None; **R. Zhang**, None; **X. Wang**, None; **G. Li**, None; **S. Qian**, None

## *References*

1. Hou R, Zhang Z, Yang D, et al. Intracranial pressure (ICP) and optic nerve subarachnoid space pressure (ONSP) correlation in the optic nerve chamber: the Beijing Intracranial and Intraocular Pressure (iCOP) study. *Brain Res*. 2016;1635:201–208.
2. Feola AJ, Myers JG, Raykin J, et al. Finite element modeling of factors influencing optic nerve head deformation due to intracranial pressure. *Invest Ophthalmol Vis Sci*. 2016;57:1901–1911.
3. Feola AJ, Coudrillier B, Mulvihill J, et al. Deformation of the lamina cribrosa and optic nerve due to changes in cerebrospinal fluid pressure. *Invest Ophthalmol Vis Sci*. 2017;58:2070–2078.
4. Bellezza AJ, Rintalan CJ, Thompson HW, Downs JC, Hart RT, Burgoyne CF. Deformation of the lamina cribrosa and anterior scleral canal wall in early experimental glaucoma. *Invest Ophthalmol Vis Sci*. 2003;44:623–637.
5. Grytz R, Meschke G, Jonas JB. The collagen fibril architecture in the lamina cribrosa and peripapillary sclera predicted by a computational remodeling approach. *Biomech Model Mechan*. 2011;10:371–382.
6. Yang H, Ren R, Lockwood H, et al. The connective tissue components of optic nerve head cupping in monkey experimental glaucoma part 1: global change. *Invest Ophthalmol Vis Sci*. 2015;56:7661–7678.
7. Ivers KM, Yang H, Gardiner SK, et al. In vivo detection of laminar and peripapillary scleral hypercompliance in early monkey experimental glaucoma. *Invest Ophthalmol Vis Sci*. 2016;57:T388–T403.
8. Li L, Bian A, Cheng G, Zhou Q. Posterior displacement of the lamina cribrosa in normal-tension and high-tension glaucoma. *Acta Ophthalmol*. 2016;94:e492–e500.
9. Girard MJA, Beotra MR, Chin KS, et al. In vivo 3-dimensional strain mapping of the optic nerve head following intraocular

pressure lowering by trabeculectomy. *Ophthalmology*. 2016; 123:1190–1200.

10. Sigal IA, Flanagan JG, Ethier CR. Factors influencing optic nerve head biomechanics. *Invest Ophthalmol Vis Sci*. 2005; 46:4189–4199.
11. Hasaneen NA. Cyclic mechanical strain-induced proliferation and migration of human airway smooth muscle cells: role of EMMPRIN and MMPs. *FASEB J*. 2005;19:1507–1509.
12. Blaauboer ME, Smit TH, Hanemaaijer R, Stoop R, Everts V. Cyclic mechanical stretch reduces myofibroblast differentiation of primary lung fibroblasts. *Biochem Bioph Res Co*. 2011;404:23–27.
13. Hinz B, Mastrangelo D, Iselin CE, Chaponnier C, Gabbiani G. Mechanical tension controls granulation tissue contractile activity and myofibroblast differentiation. *Am J Pathol*. 2001; 159:1009–1020.
14. Qu J, Chen H, Zhu L, et al. High-magnitude and/or high-frequency mechanical strain promotes peripapillary scleral myofibroblast differentiation. *Invest Ophthalmol Vis Sci*. 2015;56:7821.
15. Huang D, Liu Y, Huang Y, et al. Mechanical compression upregulates MMP9 through SMAD3 but not SMAD2 modulation in hypertrophic scar fibroblasts. *Connect Tissue Res*. 2014;55:391–396.
16. Huang X, Yang N, Fiore VF, et al. Matrix stiffness-induced myofibroblast differentiation is mediated by intrinsic mechanotransduction. *Am J Resp Cell Mol*. 2012;47:340–348.
17. Liu J, Yu W, Liu Y, et al. Mechanical stretching stimulates collagen synthesis via down-regulating SO2/AAT1 pathway. *Sci Rep UK*. 2016;6:21112.
18. O'Callaghan CJ, Williams B. Mechanical strain-induced extracellular matrix production by human vascular smooth muscle cells: role of TGF-beta (1). *Hypertension*. 2000;36:319–324.
19. Girard MJ, Suh JK, Bottlang M, Burgoyne CF, Downs JC. Biomechanical changes in the sclera of monkey eyes exposed to chronic IOP elevations. *Invest Ophthalmol Vis Sci*. 2011; 52:5656–5669.
20. Jiang L, Sun Z, Chen X, et al. Cells sensing mechanical cues: stiffness influences the lifetime of cell-extracellular matrix interactions by affecting the loading rate. *ACS Nano*. 2015;10: 207–217.
21. Tomasek JJ, Gabbiani G, Hinz B, Chaponnier C, Brown RA. Myofibroblasts and mechano-regulation of connective tissue remodelling. *Nat Rev Mol Cell Biol*. 2002;3:349–363.
22. Coudrillier B, Tian J, Alexander S, Myers KM, Quigley HA, Nguyen TD. Biomechanics of the human posterior sclera: age- and glaucoma-related changes measured using inflation testing. *Invest Ophthalmol Vis Sci*. 2012;53:1714–1728.
23. Nguyen C, Cone FE, Nguyen TD, et al. Studies of scleral biomechanical behavior related to susceptibility for retinal ganglion cell loss in experimental mouse glaucoma. *Invest Ophthalmol Vis Sci*. 2013;54:1767–1780.
24. Meyer-ter-Vehn T, Sieprath S, Katzenberger B, Gebhardt S, Grehn F, Schlunck GN. Contractility as a prerequisite for tGF-β-induced myofibroblast transdifferentiation in human tenon fibroblasts. *Invest Ophthalmol Vis Sci*. 2006;47:4895–4904.
25. Liu L, Li H, Cui Y, et al. Calcium channel opening rather than the release of ATP causes the apoptosis of osteoblasts induced by overloaded mechanical stimulation. *Cell Physiol Biochem*. 2017;42:441–454.

Investigative Ophthalmology & Visual Science